Neurol Ther (2025) 14:357–377
https://doi.org/10.1007/s40120-024-00691-w

ORIGINAL RESEARCH

Safety, Tolerability and Pharmacokinetic-Pharmacodynamic Relationship of NX210c Peptide in Healthy Elderly Volunteers: Randomized, Placebo-Controlled, Double-Blind, Multiple Ascending Dose Study

Annette Janus · Daniël Dumas · Juliette Le Douce · Sébastien Marie · Giuseppe Pasculli · Pauline Bambury · Sighild Lemarchant · Philip Kremer · Yann Godfrin

Received: October 9, 2024 / Accepted: November 26, 2024 / Published online: December 21, 2024
© The Author(s) 2024

ABSTRACT

Introduction: Blood-brain barrier (BBB) integrity is fundamental to brain homeostasis, enabling control of substance exchange and safeguarding neurons against harmful toxins, pathogens, and immune cells that lead to dysregulation and inflammation involved in ageing and neurodegenerative diseases (NDD). The cyclized peptide NX210c is a thrombospondin type 1 repeat analogue derived from subcommissural organ-spondin. It exerts beneficial effects in animal models of NDD owing to its effects on neurons and endothelial cells. NX210c demonstrated a good safety profile in a single ascending dose phase 1a clinical study. The present multiple ascending dose phase 1b study was performed to evaluate the tolerability and pharmacological effects of repeated doses of NX210c in healthy elderly (age: > 55 years) volunteers.

Methods: This was a randomized, placebo-controlled, double-blind study (EudraCT No. 2022-002868-76), investigating safety/tolerability, pharmacokinetics, and pharmacodynamics (including blood and cerebrospinal fluid biomarkers). Participants received 5 or 10 mg/kg NX210c or placebo (10-min infusion) thrice weekly for 4 weeks in an ascending dose fashion. Follow-up was conducted 2 weeks after last dosing.

Results: The investigation included 29 participants. No serious adverse events were recorded and all adverse events were mild. Dedicated

Prior Presentation: This manuscript is based on work that was partly presented at the Neuroscience 2023 annual meeting (November 11–15) in Washington, DC, USA (poster), and at AD/PD™ 2024, International Conference on Alzheimer's and Parkinson's Diseases and related neurological disorders (March 5–9) in Lisbon, Portugal (oral).

Annette Janus and Daniël Dumas have contributed equally to this work.

A. Janus (✉) · J. Le Douce · S. Marie · S. Lemarchant · Y. Godfrin
Axoltis Pharma, Bioparc Laennec, 60 Avenue Rockefeller, 69008 Lyon, France
e-mail: ajanus@axoltis.com

D. Dumas · P. Kremer
Centre for Human Drug Research (CHDR), Leiden, The Netherlands

D. Dumas · P. Kremer
Leiden University Medical Centre (LUMC), Leiden, The Netherlands

G. Pasculli · P. Bambury
InSilicoTrials Technologies, Trieste, Italy

Y. Godfrin
Godfrin Life-Sciences, Caluire-Et-Cuire, France

central nervous system testing did not reveal neurotoxicity. Biomarker evaluation showed a statistically significant reduction in blood claudin-5 and a trend toward reduction of blood homocysteine. In silico data modelling revealed salient pharmacokinetic-pharmacodynamic relationships, including reduction of claudin-5, neurofilament light chain, and SPARC-like protein 1 release, and degradation of homocysteine.
***Conclusion*:** Multiple doses of NX210c exhibited a good safety profile, showed non-cumulative pharmacokinetics, and exerted pharmacodynamic effects on biomarkers linked to BBB integrity. The effects of NX210c on claudin-5 and biomarkers influencing BBB integrity—and the overarching brain protection it offers—provide a novel therapeutic strategy targeting an underlying driver of neurodegenerative conditions for which disease-modifying treatments are limited or not available.

Keywords: NX210c peptide; Subcommissural organ-spondin; Neurodegenerative disease; Blood-brain barrier; Claudin-5; Homocysteine; Neurofilament light chain; Thrombospondin-1 analog

Key Summary Points

Why carry out this study?
Neurodegenerative diseases are responsible for irreversible decline in cerebral function; disease progression results in ongoing impairment of neurological function, leading to disability
Given the increase in neurodegenerative disease prevalence globally and the limited effective treatments available, there is an urgent need to investigate novel therapeutic targets and consider innovative approaches in this area
This phase 1b study investigated the safety and effects of multiple intravenous infusions of NX210c in healthy elderly volunteers to advance understanding of its potential utility in neurodegenerative diseases, such as amyotrophic lateral sclerosis
What was learned from the study?
Treatment using multiple doses of NX210c showed a good safety profile in healthy elderly volunteers and exerted pharmacodynamic effects on biomarkers linked to blood-brain barrier integrity, neuroprotection, and synaptic function
Treatment with NX210c reduces plasma claudin-5 (the most prominent structural tight junction protein), supporting its implication in the restoration mechanism of the blood-brain barrier integrity
In silico modelling applies differential analytics to a given dataset and offers supplemental information regarding NX210c, which can be used to inform conclusions and decision-making for phase 2 and further clinical trials

INTRODUCTION

Neurodegenerative diseases (NDD), such as amyotrophic lateral sclerosis (ALS), Alzheimer's disease, multiple sclerosis, Parkinson's disease, and Huntington's disease, involve progressive deterioration of neuronal structures, function, and ultimately loss of neurons [1, 2]. The substantial societal implications of this group of diseases have become a prominent healthcare challenge. Similarly, secondary neurodegeneration may accompany diseases, including multiple sclerosis, stroke, and neurotraumas. Although current pharmacological options for neurodegeneration may delay symptoms and/or impairments in patients, they remain non-curative [1, 3–5]; thus, innovative therapeutics and methods are required to advance treatment in this area.

Blood-brain barrier (BBB) permeability [6], neuroinflammation [7], synapse derangement [8], and genetic factors contribute to the complexity

and propagation of neuronal injury [9, 10]. The BBB, composed of microvascular endothelial cells and their tight junctions, pericytes, astrocytic terminal processes, and adjacent basement membranes, protects and regulates exchange to/from the central nervous system (CNS). Disruption of brain vessel endothelial tight junctions, especially claudin-5, alters BBB permeability, allowing access to the CNS and entry of systemic circulation constituents that have a potential to trigger or perpetuate degeneration through inflammation, oxidative stress, and excitotoxicity [11–13]. Thus, claudin-5 is increased in the blood stream in case of BBB impairment. BBB integrity decreases with age [14–17] and its loss has been associated with vascular dementia [9], ALS [18], multiple sclerosis [19], and Huntington's disease [20]. Moreover, it underlies the progression of many NDD [21–23] and may even precede disease development (e.g., Alzheimer's disease, ALS, Huntington's disease) [15, 24, 25]. Restoring BBB integrity could safeguard cerebral function to hinder/halt neurodegenerative progression or support recovery from disability [23].

NX210c is a chemically synthesized peptide composed of 12 amino acids. It is designed from the most conserved sequence of the type 1 thrombospondin repeats (TSR1) of the subcommissural organ-spondin (SCO-spondin) [26], a glycoprotein secreted during embryogenesis with important involvement in axonal guidance and BBB maintenance [27, 28]. In vitro and in vivo preclinical proof-of-concept studies have shown that NX210c improved the integrity of mouse and human BBB with evidence of reduction of the BBB permeability linked to increased claudin-5 and occludin expression on endothelial cells, resulting in increased trans-endothelial electrical resistance and decreased endothelial cell permeability [29]. Moreover, NX210c protected neurons from neurodegeneration [30] and enhanced synaptic transmission between neurons in models of synaptic dysfunction induced by phencyclidine [30] or glucose/oxygen deprivation [31].

NX210c exhibited an excellent safety profile in a single ascending dose phase 1a study involving healthy volunteers [32]. Therefore, in this phase 1b study, a healthy elderly (age: > 55 years) volunteer population was targeted to evaluate the safety/tolerability and pharmacological effects of multiple ascending doses of NX210c.

METHODS

Study Design

This was a double-blind, randomized, placebo-controlled, multiple ascending dose trial in healthy elderly volunteers (ClinicalTrials.gov Identifier: NCT05827653) conducted at The Center for Human Drug Research (CHDR, Leiden, The Netherlands) (Fig. 1).

The study duration was up to 124 days (≤ 84 days for screening, 26 days of treatment, and 14 days of washout before follow-up evaluation).

This clinical study was conducted in full compliance with the protocol, principles of the Declaration of Helsinki, the International Council for Harmonization of Technical Requirements for Pharmaceuticals for Human Use Good Clinical Practice guidelines, and the laws and regulations of France and The Netherlands. The study was approved by the Independent Ethics Committee (Medisch Ethische ToetsingsCommissie) of the Foundation 'Evaluation of Ethics in Biomedical Research' (Stichting Beoordeling Ethiek Biomedisch Onderzoek), Assen, The Netherlands.

Participants

All participants provided written informed consent prior to their participation. The main inclusion criteria for participants were: (1) healthy adults; (2) age: ≥ 55 years; (3) maximum weight: 110 kg; (4) body mass index: 18–32 kg/m^2; (5) a Mini-Mental State Examination score ≥ 25 at screening.

Interventions

Two doses of NX210c (i.e., 5 and 10 mg/kg) were investigated in this study. NX210c was prepared in glucose 5% at a concentration of 10 mg/ml for intravenous infusion of 5 mg/kg (cohort 1)

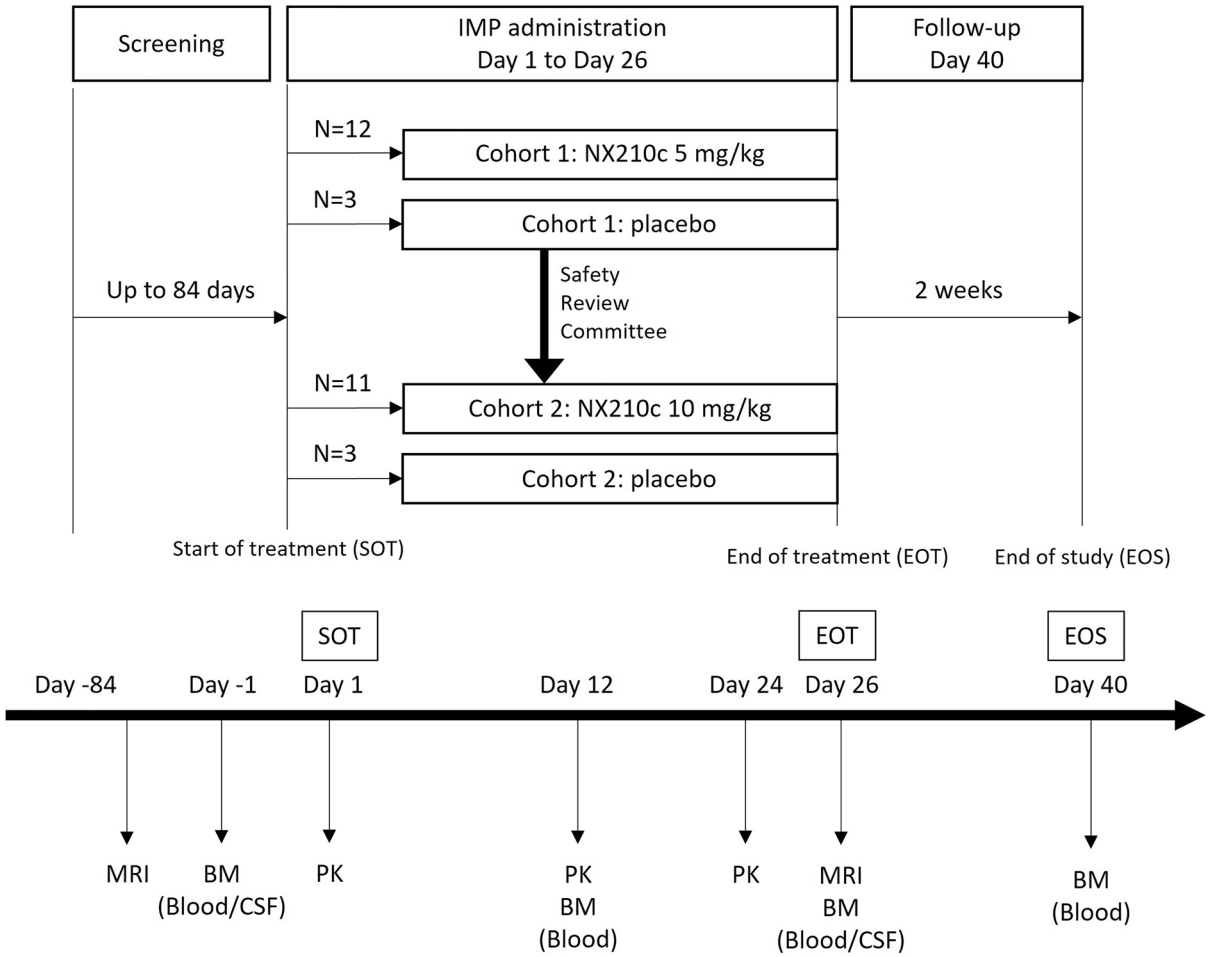


Fig. 1 Study design and main assessment. *BM* biomarker, *CSF* cerebrospinal fluid, *IMP* investigational medicinal product, *MRI* magnetic resonance imaging, *PK* pharmacokinetic

or 10 mg/kg (cohort 2) within 10 min. The comparative drug (placebo) was glucose 5% for intravenous infusion within 10 min. Treatment was administered thrice weekly for 4 weeks. Follow-up was conducted 2 weeks after last dosing.

Assessment Parameters

The primary objective of this study was to assess the safety and tolerability of multiple doses of NX210c. The assessment included the severity and incidence of treatment-emergent adverse events (AE), serious AE, suspected unexpected serious adverse reactions, infusion-related reactions, clinical laboratory tests, electrocardiography parameters (heart rate, PR interval, QRS duration, QT interval, and corrected QT interval by Fredericia), vital signs, and physical and neurological examination at screening, after each administration, and at the end of the study (2-week follow-up). A safety and review committee analyzed the safety and pharmacokinetic (PK) data for dose escalation recommendation.

The secondary objectives were as follows. First, we sought to determine the PK profile of NX210c in plasma after multiple doses. Thus, we measured and calculated the maximum concentration (C_{max}), time at which C_{max} was observed (T_{max}), area under the curve (AUC) up to the last measurable concentration (AUC

$_{0–last}$), AUC to infinite time ($AUC_{0–inf}$), half-life ($t½$), total clearance (CL), and volume of distribution (Vz). Blood was drawn on days 1, 12, and 24 at pre-dose and 5, 10, 15, 20, 40, and 80 min after treatment in dipotassium ethylenediaminetetraacetic acid (K_2EDTA) tubes (manufacturer reference: 368,861; Becton Dickinson, Franklin Lakes, NJ, USA). While on ice, the samples were transferred to a precooled Low Protein Binding Tube containing orthophosphoric acid (Merck Chemicals Gmbh, Darmstadt, Germany) and Halt™ Protease and Phosphatase Inhibitor Cocktail (Thermo Fisher Scientific, Waltham, MA, USA). Finally, after centrifugation for 10 min at 2000×g at + 2–8 °C, the plasma samples were stored at − 80 °C in a solution containing orthophosphoric acid and glycerol (Merck Chemicals Gmbh). The concentration of NX210c was determined using liquid chromatography-tandem mass spectrometry (QPS, Groningen, The Netherlands).

Second, we evaluated the presence of NX210c in the cerebrospinal fluid (CSF). CSF was drawn on day 1 (baseline) and 20 min after treatment on day 26. The samples were treated with the same reagents as for blood and analyzed by liquid chromatography-tandem mass spectrometry.

Finally, for further clinical development in patients, we investigated appropriate doses of NX210c for dose recommendation based on safety, pharmacological effects, and the pharmacokinetic-pharmacodynamic (PKPD) relationship.

Exploratory objectives included a deeper investigation of neuro-tolerability, and changes in blood and CSF biomarkers. First, NeuroCart® (CHDR) (https://chdr.nl/clinical-studies-development/methods-biomarkers/central-nervous-system/neurocart), a battery of neurophysiological tests, was utilized to evaluate potential side effects of NX210c on functional domains of the CNS, including eye movements, body sway evaluation, and performance of electroencephalogram (EEG) (i.e., capturing waveforms in select brain regions). EEG analysis was performed using the International 10–20 system, with an eyes close/opened paradigm capturing gamma, beta, alpha, theta, and delta bands at each of the following electrode positions Fz-Cz, Pz-O1, and Pz-O2, and power spectral density assessed [33]. In addition, magnetic resonance imaging (MRI) (Leiden University Medical Centre, Leiden, The Netherlands) was used to evaluate changes between pre-treatment and day 26 imaging integrity, cerebral blood flow, and BBB permeability. The method involved a bolus injection of 0.5 mmol/ml gadoterate meglumine (Clariscan™, GE HealthCare, Chicago, IL, USA) for dynamic contrast-enhanced MRI and the measurement of Ki. Arterial spin labelling MRI was used to explore the effects of NX210c on cerebral blood flow as a pharmacodynamic biomarker of potential efficacy. Second, changes in blood and CSF biomarkers were evaluated to detect the pharmacological effects of NX210c. Blood was drawn in K_2EDTA tubes on day − 1 (baseline), 12, and 26 prior to dosing and at day 40. CSF was collected via lumbar puncture at baseline and day 26 (10 min after the end of administration). The concentration of biomarkers was determined by enzyme-linked immunosorbent assay (i.e., claudin-5, neurofilament light chain [NfL], vascular cell adhesion molecule (VCAM) and SPARC-like protein 1 [SPARCL1]) (KCas Bio Europe, Lyon, France), high-performance liquid chromatography (i.e., homocysteine or tryptophan) (Hospices Civils de Lyon, Lyon, France), or biochemistry for albumin and immunoglobulin G (IgG) to calculate the CSF/serum quotient of albumin (Qalb) and CSF/serum quotient of IgG (QIgG).

Statistical Analysis and Modelling

All safety and statistical analyses were conducted with SAS 9.4 for Windows or newer (SAS Institute Inc., Cary, NC, USA). PK variable analyses were conducted with R 3.6.1 for Windows or newer (R Foundation for Statistical Computing/R Development Core Team, 2019, Vienna, Austria).

Data management, tabulation, and visualization, as well as exposure–response analyses were performed using the R statistical software, version 4.2.1. A statistical analysis of the estimated least-square means between the treatment groups and placebo group was undertaken, also focusing on some specific subgroups of age.

Conventional statistical analysis included the following datasets: prespecified (overall population) and subgroup (age: 55–70 and > 70 years) analysis and a post hoc analysis including the follow-up period.

PK modelling involved one- and two-compartment models with varied inputs, and elimination functions were examined in accordance with previous population PK models of peptides [34]. Target-mediated drug disposition (TMDD) offered a comprehensive and mechanistic understanding of drug behaviour [35, 36] and a log-normal distribution assumed for individual PK parameters for tested models.

To describe the concentration-time profile of NX210c, various PK model structures were evaluated, including one- and two-compartment models with different input and elimination functions, tailored to describe the PK of peptides [34]. Additionally, TMDD models were tested to capture drug-target dynamics for influences on drug PK [35, 36].

PKPD modelling assessed the impact of NX210c on a data-driven subset of blood biomarkers associated with BBB integrity, neuroinflammation, synaptic transmission, and neurodegeneration. Given previous evidence of a delay between the appearance of NX210c in plasma and its effects on blood biomarkers, indirect response models using ordinary differential equations were used to consider these delayed effects [37]. In these models, PD response assumes equilibrium between release and degradation in the absence of treatment, with treatment influencing either process through stimulation or reduction.

PK and PD models were developed using a population approach, incorporating fixed effects to quantify the typical behaviour within the population and random effects to account for inter-individual variability. Participant baseline characteristics, such as age, sex, or body mass index, were tested as covariates to evaluate their potential in explaining the variability between participants [38].

Model parameters were estimated using the Stochastic Approximation Expectation Maximization Algorithm [39] in Monolix software (version 4.2.2; Lixoft, Antony, France). The Conditional Sampling use for Stepwise Approach based on Correlation tests (COSSAC) algorithm [40] in Monolix was used to identify possible parameter-covariate relationships. Population PK parameters were first estimated using NX210c plasma concentrations. Subsequently, population PD parameters were estimated using an intermediate approach [41], in which population PK parameters were fixed to their previously estimated values, and individual PK parameters were sampled from their conditional distributions. Model development criteria included the corrected Bayesian information criteria (cBIC) from Monolix, the precision of parameter estimates, and the physiological relevance of the model. Graphical diagnostics such as observations versus predictions, residual scatter plots, and Visual Predictive Checks further informed the appropriateness of the model.

The PKPD relationship for SPARCL1 was utilized for precision dose modelling at concentrations of 2.5, 5, 7.5, and 10 mg/kg NX210c, simulating individual participant profiles (1 virtual participant per dose; weight: 75 kg; age: 70 years) and also a population of 200 virtual participants per dose; the latter was used in all dosing schemes, simulating crossover design. Normal data distribution was assumed, with mean and standard deviation derived from the phase 1b dataset.

RESULTS

Participants

A total of 29 participants were enrolled and completed the study. Of those, 12, 11, and 6 participants received 5 mg/kg NX210c, 10 mg/kg NX210c, and placebo, respectively. The mean age of all participants was 68.8 (range 56–91) years (Table 1). Treatment compliance was 99% across all arms. All participants completed this study.

Safety and Tolerability

A total of 73 treatment-emergent AE were recorded (Table 2). Of those, 16, 51, and 6 treatment-emergent AEs occurred in 7 participants

Table 1 Demographics of study participants (safety population)

Characteristic	5 mg/kg NX210c $N=12$[a]	10 mg/kg NX210c $N=11$[b]	Placebo $N=6$[c]	All participants $N=29$[d]
Age (years)				
Mean (SD)	71.0 (5.7)	66.4 (7.2)	69.0 (12.7)	68.8 (8.0)
Median	70	70	67	70
Min., max	62, 83	56, 76	57, 91	56, 91
Height (cm)				
Mean (SD)	175.41 (8.34)	168.35 (10.20)	177.43 (8.90)	173.15 (9.68)
Median	173.9	163.8	177.1	173.1
Min., max	165.6, 191.7	154.3, 182.7	166.5, 188.9	154.3, 191.7
Weight (kg)				
Mean (SD)	78.354 (9.203)	70.627 (8.760)	78.400 (12.730)	75.433 (10.210)
Median	77.13	69.85	76.08	74.40
Min., max	59.00, 94.40	53.35, 83.65	66.75, 99.60	53.35, 99.60
BMI (kg/m^2)				
Mean (SD)	25.54 (3.19)	24.96 (2.86)	24.77 (2.10)	25.16 (2.79)
Median	26.5	25.7	24.6	25.7
Min., max	20.1, 29.3	20.2, 29.8	22.1, 27.9	20.1, 29.8
Sex				
Female	3 (25.0%)	8 (72.7%)	0 (0%)	11 (37.9%)
Male	9 (75.0%)	3 (27.3%)	6 (100%)	18 (62.1%)
Race				
Asian	1 (8.3%)	0 (0%)	0 (0%)	1 (3.4%)
Black or African American	0 (0%)	1 (9.1%)	0 (0%)	1 (3.4%)
White	11 (91.7%)	10 (90.9%)	6 (100%)	27 (93.1%)

BMI body mass index, *SD* standard deviation

[a]Aged 55–70 years: $N=7$; aged > 70 years: $N=5$

[b]Aged 55–70 years: $N=7$; aged > 70 years: $N=4$

[c]Aged 55–70 years: $N=3$; aged > 70 years: $N=3$

[d]Aged 55–70 years: $N=17$; aged > 70 years: $N=12$

in the 5 mg/kg treatment group, 10 participants in the 10 mg/kg treatment group, and 3 participants in the placebo group, respectively. All related AEs were mild in severity; among them, one participant in the 5 mg/kg group developed skin reaction around the injection point (grade

Table 2 Treatment-emergent adverse events (safety population)

System organ class/preferred term	5 mg/kg NX210c (*N* = 12)		10 mg/kg NX210c (*N* = 11)		Placebo (*N* = 6)	
	Events *N*	Participants *N* (%)	Events *N*	Participants *N* (%)	Events *N*	Participants *N* (%)
Any events	16	7 (58.3)	51	10 (90.9)	6	3 (50.0)
Gastrointestinal disorders	3	3 (25.0)	–	–	1	1 (16.7)
Abdominal pain	–	–	–	–	1	1 (16.7)
Diarrhea	1	1 (8.3)	–	–	–	–
Flatulence	1	1 (8.3)	–	–	–	–
Toothache	1	1 (8.3)	–	–	–	–
General disorders and administration site conditions	–	–	12	5 (45.5)	–	–
Administration site irritation	–	–	9	4 (36.4)	–	–
Fatigue	–	–	1	1 (9.1)	–	–
Infusion site pain	–	–	1	1 (9.1)	–	–
Injection site haematoma	–	–	1	1 (9.1)	–	–
Infections and infestations	2	2 (16.7)	2	2 (18.2)	1	1 (16.7)
COVID-19	1	1 (8.3)	–	–	1	1 (16.7)
Nasopharyngitis	1	1 (8.3)	1	1 (9.1)	–	–
Otitis media	–	–	1	1 (9.1)	–	–
Injury, poisoning and procedural complications	2	1 (8.3)	5	2 (18.2)	2	1 (16.7)
Infusion-related reaction	2	1 (8.3)	–	–	–	–
Post-lumbar puncture syndrome	–	–	2	2 (18.2)	–	–
Post-procedural discomfort	–	–	1	1 (9.1)	–	–
Post-procedural haematoma	–	–	–	–	2	1 (16.7)
Procedural pain	–	–	1	1 (9.1)	–	–
Wound	–	–	1	1 (9.1)	–	–
Musculoskeletal and connective tissue disorders	2	1 (8.3)	1	1 (9.1)	–	–
Back pain	–	–	1	1 (9.1)	–	–
Limb discomfort	1	1 (8.3)	–	–	–	–
Myalgia	1	1 (8.3)	–	–	–	–
Nervous system disorders	4	2 (16.7)	26	8 (72.7)	2	2 (33.3)
Headache	3	1 (8.3)	20	5 (45.5)	1	1 (16.7)
Presyncope	–	–	2	2 (18.2)	–	–

Table 2 continued

System organ class/preferred term	5 mg/kg NX210c (*N* = 12)		10 mg/kg NX210c (*N* = 11)		Placebo (*N* = 6)	
	Events *N*	Participants *N* (%)	Events *N*	Participants *N* (%)	Events *N*	Participants *N* (%)
Restless legs syndrome	1	1 (8.3)	–	–	–	–
Sensory disturbance	–	–	1	1 (9.1)	–	–
Somnolence	–	–	3	3 (27.3)	1	1 (16.7)
Psychiatric disorders	1	1 (8.3)	1	1 (9.1)	–	–
Abnormal dreams	–	–	1	1 (9.1)	–	–
Sleep disorder	1	1 (8.3)	–	–	–	–
Respiratory, thoracic, and mediastinal disorders	2	2 (16.7)	–	–	–	–
Oropharyngeal pain	1	1 (8.3)	–	–	–	–
Rhinorrhea	1	1 (8.3)	–	–	–	–
Skin and subcutaneous tissue disorders	–	–	1	1 (9.1)	–	–
Pruritus	–	–	1	1 (9.1)	–	–
Vascular disorders	–	–	3	3 (27.3)	–	–
Hot flush	–	–	2	2 (18.2)	–	–
Vasoconstriction	–	–	1	1 (9.1)	–	–

COVID-19 coronavirus disease-2019

1). Overall, there were no clinically significant electrocardiography findings.

Neurocart® Evaluation

Overall, comprehensive evaluation did not reveal statistically significant differences among the groups. However, subgroup analysis showed a 3–5% decrease in adaptive tracking performance at the higher dose and/or younger age. There were no statistically significant changes observed on EEG.

Arterial Spin Labelling and Dynamic Contrast-Enhanced MRI

The overall and subgroup by age analyses found that the whole brain K influx constant (Ki) and arterial spin labelling rate were not statistically different in the treatment groups compared with the placebo group. No structural abnormalities were detected on pre-dose MRI or changes in MRI data following treatment.

PKs

Non-compartmental analysis of NX210c PKs revealed that NX210c was rapidly eliminated with a 17–18-min half-life and did not accumulate following multiple doses (Fig. 2). Mean

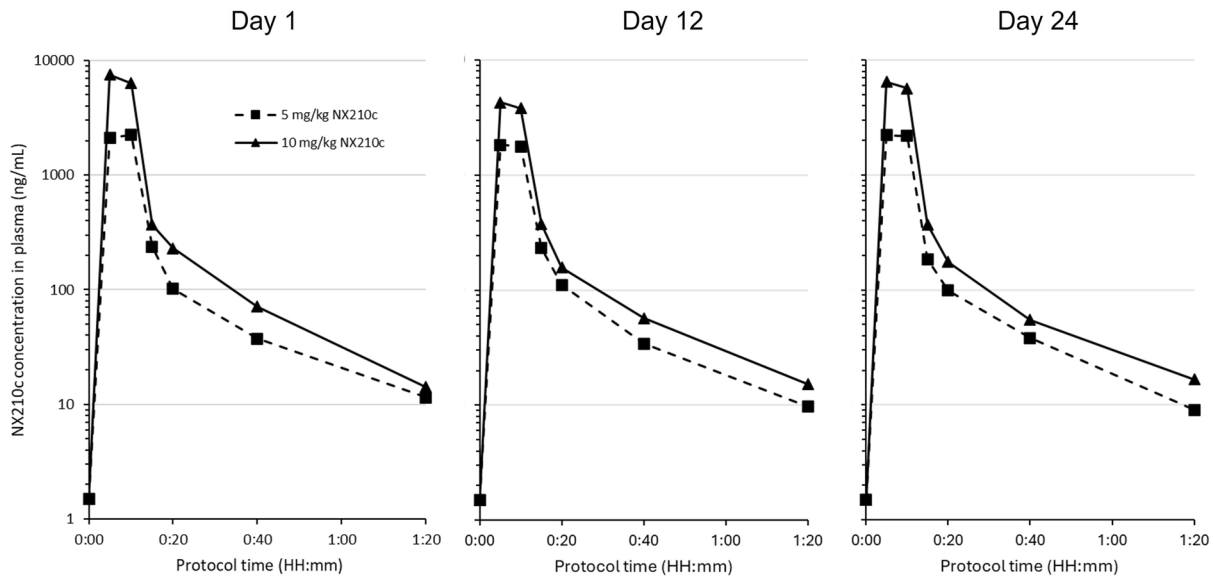


Fig. 2 NX210c concentration in the plasma on Day 1, Day 12, and Day 24 (pharmacokinetic population)

C_{max} in blood was dose proportional, ranging from 2481 ng/ml (5 mg/kg dose) to 6835 ng/ml (10 mg/kg). Similarly, exposure (AUC_{inf}) ranged from 378 h*ng/ml (5 mg/kg dose) to 908 h*ng/ml (10 mg/kg) with good tissue diffusion and clearance (Table 3). NX210c was not detectable in the CSF on day 26.

In further evaluations using population PK modelling, a two-compartment Wagner TMDD model [36] structure exhibited the best performance in terms of clinical plausibility, parameter estimates, goodness of fit, and cBIC. The Wagner TMDD two-compartment model had a lower cBIC and was selected as the final population PK model. A noteworthy observation was the obtained dissociation constant (K_D) value of 48.27 nM, which aligns well with the K_D range (1–100 nM) associated with TMDD models. The final population PK structural model (Fig. 3) was employed for the PKPD relationship modelling.

Non-linear response curves to concentrations of NX210c were observed for blood biomarkers (i.e., claudin-5, homocysteine, NfL, and SPARCL1). Indirect response models showed reduction of release curves (claudin-5, NfL, and SPARCL1) and stimulation of homocysteine degradation.

Pharmacodynamic Effects and PKPD Relationship Modelling

Claudin-5

A significant decrease in plasma claudin-5 was observed in the 5 mg/kg treatment group versus placebo throughout 26 days (−1.3264 ng/ml, $p=0.0479$). Subgroup analysis by age showed significant differences in both 5 mg/kg (−2.2539 ng/ml, $p=0.0094$) and 10 mg/kg (−1.8260 ng/ml, $p=0.0306$) treatment groups of participants aged 55–70 years with post hoc analysis in the follow-up period (over 40 days) indicating a significant, sustained decrease in claudin-5 levels in the 5 mg/kg group (−1.8955 ng/ml, $p=0.0148$) versus placebo and a trend in the 10 mg/kg group (−1.3932 ng/ml, $p=0.0644$) (changes from baseline are shown in Fig. 4).

For compartmental modelling, the sigmoidal equation used to describe the reduction of claudin-5 release by NX210c concentrations showed reduced levels of claudin-5 upon drug administration. The 80% inhibitory concentration (IC80) value for NX210c concentration was 20.20 nM, suggesting that most individuals in both treatment groups might achieve the drug

Table 3 NX210c plasma pharmacokinetic parameters (pharmacokinetic population)

Treatment	Parameter	Unit	N	Mean	Geometric mean	SD	CV (%)	Geometric CV (%)	Median	Min	Max
5 mg/kg NX210c	$AUC_{0-80\ min}$	h*ng/ml	35	378.0	350.0	147.41	39.0	42.5	357	135	629
	AUC_{inf}	h*ng/ml	30	378.8	348.6	154.32	40.7	44.3	343	140	634
	CL	L/h	30	1416.5	1282.0	646.18	45.6	48.6	1405	589	2990
	C_{max}	ng/ml	35	2481.4	2218.6	1156.89	46.6	53.0	2163	663	4683
	C_{trough}	ng/ml	23	0.0	–	0.00	–	–	0	0	0
	Vz	L	30	595.5	541.3	280.13	47.0	46.2	580	268	1369
	$t_{1/2}$	h	30	0.2993	0.2983	0.02438	8.1	8.2	0.302	0.257	0.341
	t_{max}	h	35	–	–	–	–	–	0.1100	0.0800	0.1967
10 mg/kg NX210c	$AUC_{0-80\ min}$	h*ng/ml	33	951.0	853.6	460.60	48.4	50.3	874	342	1903
	AUC_{inf}	h*ng/ml	30	908.3	823.8	422.58	46.5	47.6	877	348	1914
	CL	L/h	30	1052.4	946.4	535.99	50.9	47.7	850	488	2295
	C_{max}	ng/ml	33	6835.2	5880.3	3703.66	54.2	63.4	6363	1687	13,783
	C_{trough}	ng/ml	21	13.7	287.0	62.63	458.3	–	0	0	287
	Vz	L	30	437.6	395.1	223.24	51.0	46.1	337	215	981
	$t_{1/2}$	h	30	0.2859	0.2844	0.02956	10.3	10.8	0.293	0.229	0.330
	t_{max}	h	33	–	–	–	–	–	0.1400	0.0800	0.1400

AUC area under the curve, $AUC_{0-80\ min}$ AUC up to 80 min, AUC_{inf} AUC to infinite time, *CL* total clearance, C_{max} maximum concentration, C_{trough} trough concentration, *CV* coefficient of variation, *SD* standard deviation, *t½* half-life, t_{max} time at which C_{max} was observed, *Vz* volume of distribution

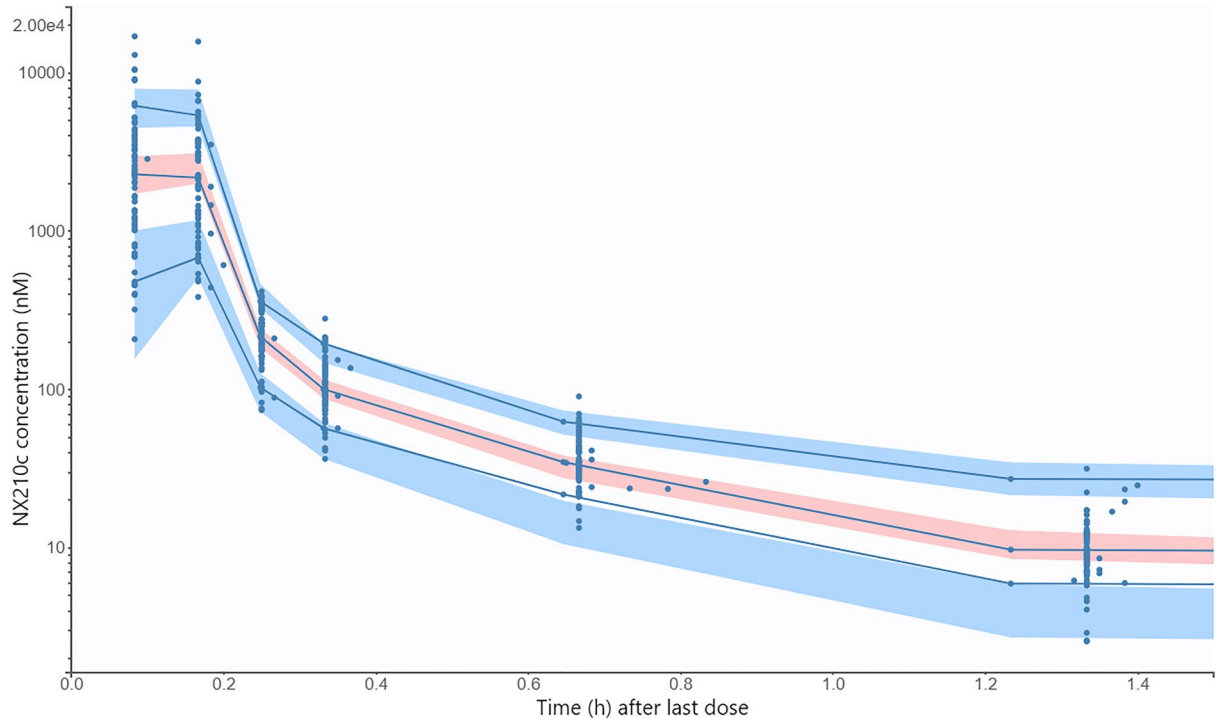


Fig. 3 Visual predictive checks for the final population pharmacokinetic model of NX210c

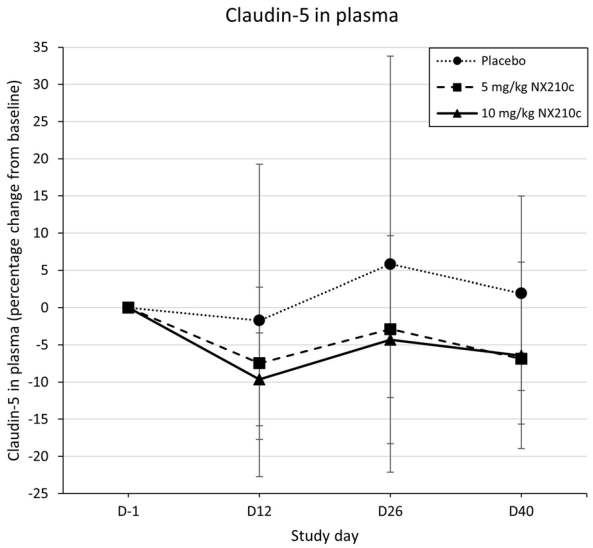


Fig. 4 Change from baseline of claudin-5 concentration in the plasma

concentration required to experience 80% of the maximal effect (Fig. 5).

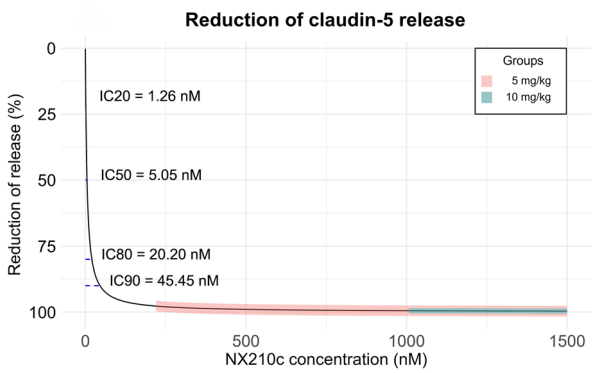


Fig. 5 Reduction of claudin-5 release by NX210c by dose groups. C_{max} maximum concentration, *IC* inhibitory concentration, *SD* standard deviation

Homocysteine

In patients aged > 70 years treated with 10 mg/kg NX210c, there was a consistent trend toward lowering of plasma homocysteine levels compared with placebo at day 26 (– 2.2 µmol/l, $p = 0.0579$) and throughout 26 days (– 2.0 µmol/l, $p = 0.0525$). Similarly,

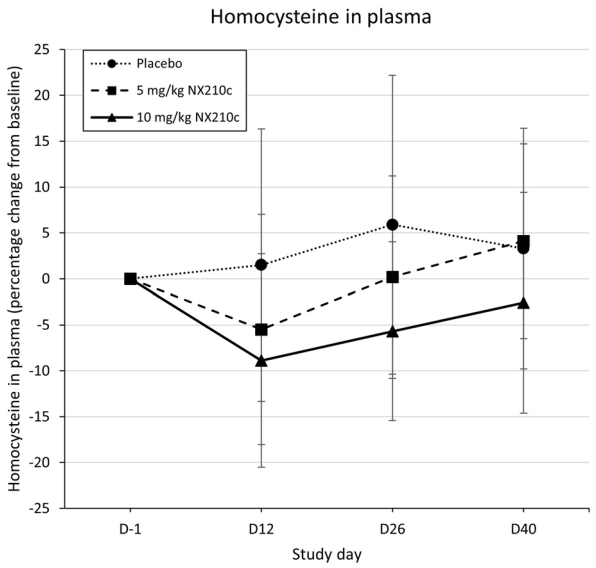


Fig. 6 Change from baseline of homocysteine concentration in the plasma

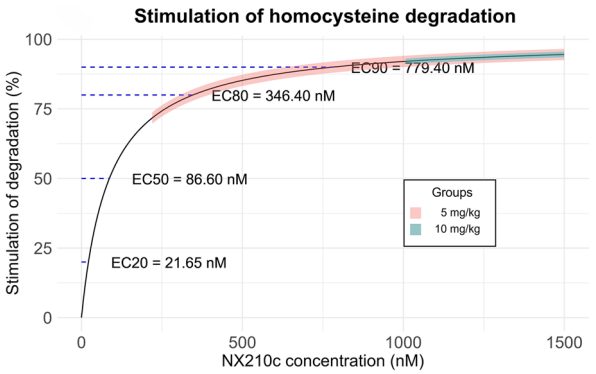


Fig. 7 Stimulation of degradation: Effect of NX210c on homocysteine degradation by dose groups. C_{max} maximum concentration, *EC* effective concentration, *SD* standard deviation

post hoc subgroup analysis by age showed a trend toward decreased plasma homocysteine levels versus placebo at day 26 (−2.1 µmol/l, $p=0.0551$) (changes from baseline are shown in Fig. 6).

A sigmoidal equation was used for stimulation of homocysteine degradation by NX210c concentrations and revealed reduced levels of homocysteine upon treatment. The 80% effective concentration (EC80) value for NX210c concentration was 346.4 nM. These results indicate that some individuals in the 5 mg/kg group may not reach the drug concentration necessary to achieve 80% of the maximal effect. However, all participants receiving 10 mg/kg are expected to attain this level of efficacy (Fig. 7).

Tryptophan

Statistical analysis at day 26 showed that tryptophan levels in plasma were significantly increased in both treatment groups (5 mg/kg: +34.6 µmol/l, $p=0.0009$; 10 mg/kg: +68.9 µmol/l, $p<0.0001$) compared with the placebo group (mean value: 57.6 µmol/l). This increase was also observed throughout 26 days in a dose-dependent manner. The subgroup analysis showed a significant increase in tryptophan levels in the CSF after treatment with 10 mg/kg NX210c versus placebo throughout 26 days (+1.0 µmol/l, $p=0.0436$), particularly in patients aged > 70 years (+2.0 µmol/l, $p=0.0154$). However, increases were no longer statistically significant by day 40 of follow-up (changes from baseline are shown in Fig. 8).

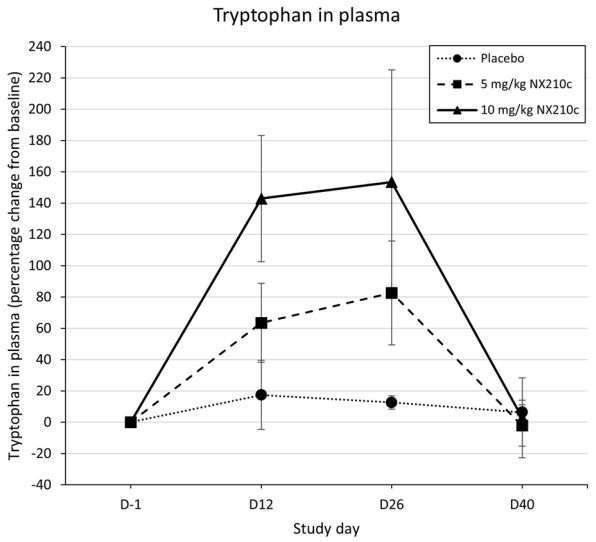


Fig. 8 Change from baseline of tryptophan concentration in the plasma

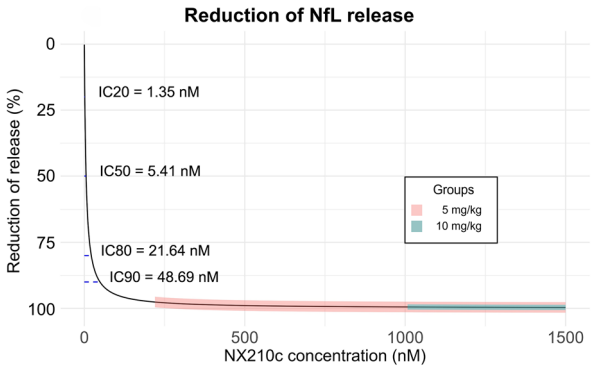


Fig. 9 Reduction of NfL release by NX210c by dose groups. C_{max} maximum concentration, *IC* inhibitory concentration, *NfL* neurofilament light chain, *SD* standard deviation

NfL

NfL levels in plasma and in the CSF did not demonstrate statistically significant differences in the treatment groups compared with the placebo group in the overall analysis. However, the PKPD relationship derived from compartmental modelling exhibited a sigmoidal-based reduction pattern on the release rate of blood NfL, revealing reduced levels related to NX210c blood concentration. The IC80 value for NX210c concentration was 21.64 nM, implying that most individuals in both treatment groups may achieve the drug concentration required to experience 80% of the maximal effect (Fig. 9).

SPARCL1

There were no statistically significant results for plasma SPARCL1. However, PKPD modelling of NX210c concentration data from participants revealed a sigmoidal effect pattern, with reduction of SPARCL1 release rate (reduced levels of SPARCL1) corresponding to increasing NX210c concentration (Fig. 10).

VCAM

VCAM showed a statistically significant decrease in the older subgroup ($p=0.0491$), which represents an approximate 44% reduction on day 26 and a trend toward sustained effect on day 40 by virtue of a 38% decrease.

Dose Modelling

Dose modelling showed that some participants in the 2.5 and 5 mg/kg groups may reach the desired IC80. However, a significant number of participants in these groups do not achieve this threshold, potentially falling short of 80% of the maximal effect. In contrast, all participants in the 7.5 and 10 mg/kg dose groups successfully reached the IC80 (Fig. 11).

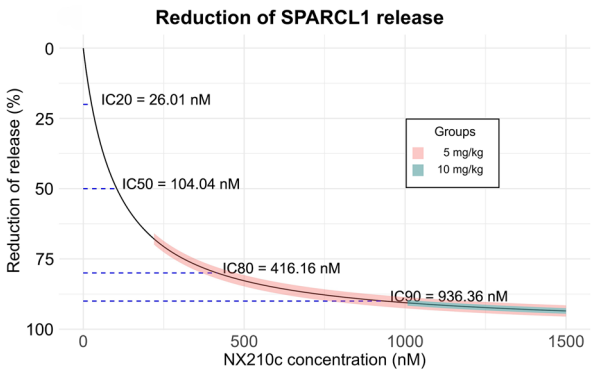


Fig. 10 Reduction of SPARCL1 release: Effect of NX210c on SPARCL1 release rate by dose groups. C_{max} maximum concentration, *IC* inhibitory concentration, *SD* standard deviation, *SPARCL1* SPARC-like protein 1

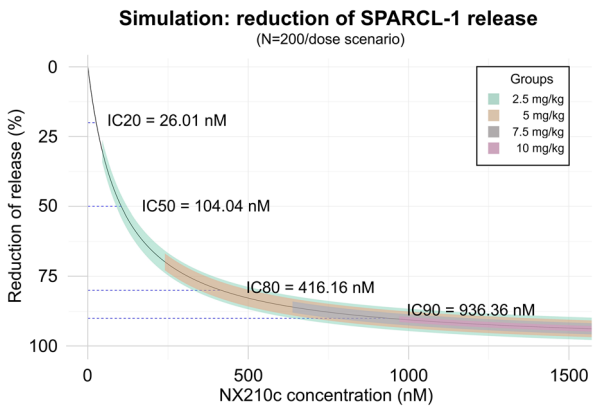


Fig. 11 Simulation (N = 200/dose scenario): Effect of NX210c on plasma SPARCL1 release rate. C_{max} maximum concentration, *IC* inhibitory concentration, *SD* standard deviation, *SPARCL1* SPARC-like protein 1

DISCUSSION

This multiple ascending dose phase 1b trial met its primary endpoint by demonstrating good safety and tolerability of NX210c, with excellent participant compliance, regardless of dose. NeuroCart® and the MRI modalities tested did not show off-target CNS pharmacological effects. All AE were mild, and plasma PK analysis showed that NX210c has a short half-life ($t½$ = 16–20 min) without accumulation in blood. Although the half-life of NX210c is short, sustained pharmacological effects have also been observed in preclinical models [29, 31, 32, 42]. However, for chronic NDD, a formulation with longer duration is under development. CSF sampling near the plasma T_{max} (blood) did not detect NX210c in the CSF, although this was probably due to sampling at the lumbosacral site. This may not adequately reflect brain parenchymal/interstitial fluid concentrations, particularly in the context of the short plasma half-life of this drug. PKPD results showed statistical significance or trends in key BBB fluid biomarkers following treatment, including sustained effects in the wash-out period. BBB alterations have been associated with ageing [14–17] in neurological diseases (including NDD) and their progression [13, 43]. Hence, in combination with its favourable benefit/risk profile, NX210c could be a promising drug in the arsenal against NDD.

Plasma claudin-5, which showed statistically significant decreases by conventional statistics as well as a PKPD relationship demonstrated through computational modelling, is key to this action (Figs. 4, 5). Furthermore, maintenance of the statistical difference over 40 days (55–70 years subgroup) after treatment with 5 mg/kg NX210c indicates a sustained effect of NX210c. Blood claudin-5 is often elevated in neurogeneration and is indicative of BBB impairment [43–45]. Therefore, reduction in blood claudin-5 levels after treatment with NX210c suggests recovery of BBB.

Homocysteine levels in plasma decreased from baseline values and showed a PKPD relationship (Figs. 6, 7). Homocysteine is a sulphur-containing amino acid and metabolite of the essential amino acid methionine. Thus, elevated homocysteine levels in plasma compromise BBB integrity by triggering vascular inflammation that leads to tight junction degradation [46] and induce synaptic dysfunction in brain parenchyma [47] via the N-methyl-D-aspartate receptor. Elevated blood homocysteine is observed in ageing [48], is associated with the risk of cognitive impairment in the elderly [16, 17, 49], and is found in patients with ALS [50, 51] and other neurological diseases [52–54]. Hence, lowering the plasma levels of homocysteine by NX210c may attenuate the circulatory environment that disrupts BBB integrity and could have substantial clinical applications.

Dose-dependent increases in blood and CSF tryptophan, an essential amino acid, were also evidenced in the study (Fig. 8). These changes could be explained by the degradation of two tryptophan residues present in the amino acid sequence of NX210c. Tryptophan is metabolized to several bioactive compounds through different metabolic pathways, which in turn participate in various physiological activities in the body and regulate body homeostasis. Tryptophan is converted into functional molecules such as serotonin and kynurenine. In situations of metabolic dysregulation, it could play a role in the nervous and immune systems [55, 56]. In our study, the observed increase in tryptophan levels did not appear to result in any AE (i.e., common and established clinical symptoms or laboratory findings). In addition, dietary tryptophan supplementation has been shown to significantly ameliorate the motor function in a rat model of Parkinson's disease [57]. Thus, an increase in tryptophan is considered an advantageous finding of potential utility in the treatment of neurological disease, particularly in case of serotonergic deficiency [58, 59].

NfL is a sensitive and dynamic protein biomarker of neuro-axonal injury [60]. Its function is to provide structural stability to neurons and enable radial growth of axons, with levels proportional to the degree of neuroaxonal injury [61]. NfL levels tend to increase with age in the blood and CSF [62, 63] and can correlate with the disease status in neurological disorders [64, 65]. Although data did not reveal a significant NfL reduction in the present study, PKPD modelling of data demonstrated a dose-dependent

lowering effect of NX210c on blood NfL levels by reduction of release. Thus, further investigation of the effect of NX210c on NfL in neurological conditions is warranted. A phase 2 trial involving patients with ALS, in whom NfL levels are significantly higher than in healthy volunteers, is currently ongoing. The results of this study may help to better understand the mechanism through which NX210c decreases blood NfL levels.

SPARCL1 is a cell matrix-modulating protein regulating synapse formation in the brain. It is highly secreted by astrocytes during CNS development and following acute CNS damage [66]. This biomarker is associated with neuroinflammatory changes observed in ageing and is closely associated with various neurological disorders [67], including chronic brain endothelial lesions [68]. In addition, increased SPARCL1 levels were shown to accelerate symptom onset in NDD [69]. Thus, the plasma SPARCL1 reduction trend maintained in the post-treatment period combined with the PKPD-modelling relationship (Fig. 10) suggests a potential effect of NX210c on the secretion of this protein by astrocytes in NDD. Furthermore, of the biomarkers exhibiting a PKPD relationship with NX210c, the SPARCL1 PKPD model afforded sensitivity and precision to guide dose selection for further clinical development based on its more gradual effect slope compared with other biomarkers with a PKPD relationship and its relevance to mechanisms under evaluation. While some participants in the 2.5 and 5 mg/kg groups may reach the desired IC80, a significant number of participants in these groups do not achieve this threshold, potentially falling short of 80% of the maximal effect. In contrast, all participants in the 7.5 and 10 mg/kg dose groups successfully reached the IC80 (Fig. 11). To minimize exposure overlap between doses considering claudin-5, homocysteine, and NfL, the maximum effect can be achieved from the 5 mg/kg dose. Considering the good safety profile of both NX210c doses, it was decided to proceed with clinical trial investigation of both doses (i.e., 5 and 10 mg/kg). This approach also considers that patients with NDD will have concomitant conditions or receive medications that could have altered response to treatment or modify the established safety and PKPD profile.

This study had certain limitations. The investigation was performed in a single centre. Hence, additional multi-centre studies are required to confirm the present findings. The encouraging results of the study may have nonetheless been impacted by several factors. In terms of demographics, the 10 mg/kg group had slightly lower mean age and mean/median weight than the other groups. In addition, a higher proportion of participants in this group were females, which could affect the generalizability of results. Differences between groups may have also been more difficult to detect considering the small sample size and relatively few time points of the study. However, in a healthy population, parameters may be unmeasurable or low; even when measurable, variability in a small placebo control arm is a constraint or adaptive mechanisms may render parameters resolute to change. For example, Qalb and QIgG in samples from healthy volunteers might limit a significant effect or detection thereof. Elevations in these parameters would indicate a breakdown of the BBB and increased permeability. These parameters did not show a significant decrease in the study; however, interestingly, the average change from baseline values was 5% lower in the NX210c groups than in the placebo group. VCAM protein is involved in the adhesion of inflammatory cells to vascular endothelium [70]. It may also be challenging to detect changes in this biomarker in a healthy population given that abnormal elevations are observed in cardiovascular conditions [71] and NDD [72], including ALS [73]. Nevertheless, despite the small sample, VCAM showed a statistically significant decrease in the older subgroup ($p=0.0491$), denoting a trend toward sustained effect.

Overall, computational modelling mitigated limitations by revealing important dose to target/effect relationships (e.g., biomarker levels), thereby enriching the results obtained from conventional statistics in the current study. Moreover, it offers insight for consideration in future trials of NX210c in NDD.

CONCLUSION

This phase 1b study demonstrated the safety and tolerability of multiple intravenous infusions of NX210c (5 and 10 mg/kg) in healthy elderly volunteers. This population was selected to determine the effects of NX210c in the ageing brain, where the initiation of neurovascular modifications could even be subclinical [11]. PK evaluation showed that this proposed thrombospondin receptor-1 analog has an approximately 18-min half-life and no accumulation when administered thrice weekly. Furthermore, statistical analysis and in silico modelling of fluid biomarker responses to treatment revealed effects related to BBB integrity and function. NX210c represents a novel therapeutic with a spectrum of disease-modifying implications relevant to causal mechanisms in NDD, including BBB repair and through an effect on mechanisms involving neuronal protection and synaptic transmission. NX210c may represent a paradigm shift in the approach to ALS; specifically, BBB alterations may even be a pre-symptomatic feature [23, 74], based on which BBB biomarker endpoints (e.g., Qalb) can be added to the arsenal of biomarker endpoints already in use (e.g., serum NfL).

Along with the available preclinical body of work, the present clinical results support the rationale for a phase 2 proof-of-concept clinical trial involving patients with ALS (NCT06365216). This study would investigate the effects and mechanism through which NX210c can promote neurovascular-regenerative processes and potentially offer further benefit to patients with a range of NDD.

ACKNOWLEDGEMENTS

The authors thank Hemme Hijma (The Centre for Human Drug Research, Leiden, The Netherlands), Dr Valérie Bourdès, Cécile Lacroix, and Alexandra Weber (Axoltis Pharma, Lyon, France) and Dr David Liens (BPLS Consulting-medical monitor), Dr Damien Colas (Bubo biosciences, Caluire et Cuire, France-EEG analysis), Dr Cécile Acquaviva and her team (LBMMS, Hospices Civiles Lyon, Lyon, France-amino acids), Dr Daniel Schulz-Jander and his team (QPS, Gröningen, The Netherlands-pharmacokinetics), Prof Thijs van Osch, Dr Jeroen van der Grond and their team (Leiden University Medical Center-MRI analysis) for their contribution to this study.

Medical Writing and Editorial Assistance. Editorial assistance in the preparation of this article was provided by Sotirios Georgantopoulos, PhD (Epimyth MedCom). Support for this assistance was funded by Axoltis Pharma.

Authorship. All named authors meet the International Committee of Medical Journal Editors (ICMJE) criteria for authorship for this article, take responsibility for the integrity of the work as a whole, and have approved the final version of this manuscript for publication.

Author Contributions. Conception of the study and/or data formatting: Daniël Dumas, Philip Kremer, Juliette Le Douce, Sébastien Marie, Sighild Lemarchant, Yann Godfrin. Study investigators: Philip Kremer (Principal), Daniël Dumas. Interpretation of the results: Annette Janus, Yann Godfrin, Daniël Dumas, Philip Kremer. PKPD modelling: Giuseppe Pasculli and Pauline Bambury. Writing of manuscript: Annette Janus, Yann Godfrin. Review of manuscript: Daniël Dumas, Juliette Le Douce, Sébastien Marie, Giuseppe Pasculli, Pauline Bambury, Sighild Lemarchant, Philip Kremer.

Funding. Sponsorship for this study was funded by Axoltis Pharma. The Region Auvergne Rhône Alpes (France), Banque Publique Investissement (BPI), and the French Ministry of Research granted funds to Axoltis Pharma supporting the project. The Rapid Service Fee was provided by Axoltis Pharma.

Data Availability. The datasets generated and/or analyzed during the current study are available from the corresponding author on reasonable request.

Declarations

Conflict of Interest. Daniël Dumas and Philip Kremer are employed by CHDR. Juliette Le Douce, Sébastien Marie, Sighild Lemarchant, and Annette Janus are employed by Axoltis Pharma. Yann Godfrin is the CEO and a shareholder of Axoltis Pharma. Giuseppe Pasculli and Pauline Bambury are employed by InSilicoTrials.

Ethical Approval. This clinical study was conducted in full compliance with the protocol, principles of the Declaration of Helsinki, the International Council for Harmonisation of Technical Requirements for Pharmaceuticals for Human Use Good Clinical Practice guidelines, and the laws and regulations of France and the Netherlands.

Open Access. This article is licensed under a Creative Commons Attribution-NonCommercial 4.0 International License, which permits any non-commercial use, sharing, adaptation, distribution and reproduction in any medium or format, as long as you give appropriate credit to the original author(s) and the source, provide a link to the Creative Commons licence, and indicate if changes were made. The images or other third party material in this article are included in the article's Creative Commons licence, unless indicated otherwise in a credit line to the material. If material is not included in the article's Creative Commons licence and your intended use is not permitted by statutory regulation or exceeds the permitted use, you will need to obtain permission directly from the copyright holder. To view a copy of this licence, visit http://creativecommons.org/licenses/by-nc/4.0/.

REFERENCES

1. Lamptey RNL, Chaulagain B, Trivedi R, Gothwal A, Layek B, Singh J. A review of the common neurodegenerative disorders: current therapeutic approaches and the potential role of nanotherapeutics. Int J Mol Sci. 2022;23:1851.

2. Wilson DM 3rd, Cookson MR, Van Den Bosch L, Zetterberg H, Holtzman DM, Dewachter I. Hallmarks of neurodegenerative diseases. Cell. 2023;186:693–714.

3. Mead RJ, Shan N, Reiser HJ, Marshall F, Shaw PJ. Amyotrophic lateral sclerosis: a neurodegenerative disorder poised for successful therapeutic translation. Nat Rev Drug Discov. 2023;22:185–212.

4. Jiang A, Handley RR, Lehnert K, Snell RG. From pathogenesis to therapeutics: a review of 150 years of Huntington's disease research. Int J Mol Sci. 2023;24:13021.

5. Zhang J, Zhang Y, Wang J, Xia Y, Zhang J, Chen L. Recent advances in Alzheimer's disease: mechanisms, clinical trials and new drug development strategies. Signal Transduct Target Ther. 2024;9:211.

6. Hussain B, Fang C, Chang J. Blood-brain barrier breakdown: an emerging biomarker of cognitive impairment in normal aging and dementia. Front Neurosci. 2021;15:1–22.

7. Ownby RL. Neuroinflammation and cognitive aging. Curr Psychiatry Rep. 2010;12:39–45.

8. Zhu Z, Zeng Q, Kong L, et al. Altered spontaneous brain activity in subjects with different cognitive states of biologically defined Alzheimer's disease: a surface-based functional brain imaging study. Front Aging Neurosci. 2021;13: 683783.

9. Sweeney MD, Sagare AP, Zlokovic BV. Blood-brain barrier breakdown in Alzheimer disease and other neurodegenerative disorders. Nat Rev Neurol. 2018;143:133–50.

10. Rasmussen MK, Mestre H, Nedergaard M. The glymphatic pathway in neurological disorders. Lancet Neurol. 2018;17:1016–24.

11. Knox EG, Aburto MR, Clarke G, Cryan JF, O'Driscoll CM. The blood-brain barrier in aging and neurodegeneration. Mol Psychiatry. 2022;27:2659–73.

12. Martin M, Vermeiren S, Bostaille N, et al. Engineered Wnt ligands enable blood–brain barrier repair in neurological disorders. Science. 2022;375: eabm4459.

13. Sweeney MD, Zhao Z, Montagne A, Nelson AR, Zlokovic BV. Blood-brain barrier: from physiology to disease and back. Physiol Rev. 2019;99:21–78.

14. Cao Y, Xu W, Liu Q. Alterations of the blood-brain barrier during aging. J Cereb Blood Flow Metab. 2024;44:881–95.

15. Montagne A, Barnes SR, Sweeney MD, et al. Blood-brain barrier breakdown in the aging human hippocampus. Neuron. 2015;85:296–302.

16. Verheggen ICM, de Jong JJA, van Boxtel MPJ, et al. Increase in blood-brain barrier leakage in healthy, older adults. Geroscience. 2020;42:1183–93.

17. Verheggen ICM, de Jong JJA, van Boxtel MPJ, et al. Imaging the role of blood-brain barrier disruption in normal cognitive ageing. Geroscience. 2020;42:1751–64.

18. Klose V, Jesse S, Lewerenz J, et al. Blood–CSF barrier integrity in amyotrophic lateral sclerosis. Brain. 2024. https://doi.org/10.1093/brain/awae144.

19. Oghabian MA, Fatemidokht A, Haririchian MH. Quantification of blood-brain-barrier permeability dysregulation and inflammatory activity in MS lesions by dynamic-contrast enhanced MR imaging. Basic Clin Neurosci. 2022;13:117–28.

20. Drouin-Ouellet J, Sawiak SJ, Cisbani G, et al. Cerebrovascular and blood-brain barrier impairments in Huntington's disease: potential implications for its pathophysiology. Ann Neurol. 2015;78:160–77.

21. Montagne A, Nation DA, Sagare AP, et al. APOE4 leads to blood-brain barrier dysfunction predicting cognitive decline. Nature. 2020;581:71–6.

22. van de Haar HJ, Burgmans S, Jansen JF, et al. Blood-brain barrier leakage in patients with early Alzheimer disease. Radiology. 2016;281:527–35.

23. Steinruecke M, Lonergan MR, Selvaraj BT, Chandran S, Diaz-Castro B, Stavrou M. Blood–CNS barrier dysfunction in amyotrophic lateral sclerosis: proposed mechanisms and clinical implications. J Cereb Blood Flow Metab. 2023;43:642–54.

24. Alarcan H, Al Ojaimi Y, Lanznaster D, et al. Taking advantages of blood-brain or spinal cord barrier alterations or restoring them to optimize therapy in ALS? J Pers Med. 2022;12:1071.

25. Che J, Sun Y, Deng Y, Zhang J. Blood-brain barrier disruption: a culprit of cognitive decline? Fluids Barriers CNS. 2024;21:63.

26. Gobron S, Monnerie H, Meiniel R, et al. SCO-spondin: a new member of the thrombospondin family secreted by the subcommissural organ is a candidate in the modulation of neuronal aggregation. J Cell Sci. 1996;109:1053–61.

27. Sepúlveda V, Maurelia F, González M, Aguayo J, Caprile T. SCO-spondin, a giant matricellular protein that regulates cerebrospinal fluid activity. Fluids Barriers CNS. 2021;18:45.

28. Gao Y, Xu J, Li S, et al. Spatial and single-cell transcriptomics on SSPO PTV mutant mice reveals SCO-spondin's function in mood regulation through brain barriers. medRxiv. 2024. https://doi.org/10.1101/2024.04.09.24305433.

29. Greene C, Rebergue N, Fewell G, et al. NX210c drug candidate peptide strengthens mouse and human blood-brain barriers. Fluids Barriers CNS. 2024;21:76.

30. Lemarchant S, Sourioux M, Le Douce J, et al. NX210c peptide promotes glutamatergic receptor-mediated synaptic transmission and signaling in the mouse central nervous system. Int J Mol Sci. 2022;23:8867.

31. Sourioux M, Lemarchant S, Le Douce J, Hugues S, Farinelli M, Godfrin Y. A subcommissural organ-spondin-derived peptide (NX210c) improves the recovery of synaptic transmission after in vitro ischemia: poster presentations. J Cereb Blood Flow Metab. 2022;42:108–273.

32. Bourdès V, Dogterom P, Aleman A, et al. Safety, tolerability, pharmacokinetics and initial pharmacodynamics of a subcommissural organ-spondin-derived peptide: a randomized, placebo-controlled, double-blind, single ascending dose first-in-human study. Neurol Ther. 2022;11:1353–74.

33. Prins S, Borghans L, de Kam ML, Groeneveld GJ, van Gerven J. Cognitive performance in healthy clinical trial participants and patients with the NeuroCart, a neurodegenerative disease measured with an automated neuropsychological and neurophysiological test battery. J Neurol Sci. 2023;449:120658.

34. Diao L, Meibohm B. Pharmacokinetics and pharmacokinetic-pharmacodynamic correlations of therapeutic peptides. Clin Pharmacokinet. 2013;52:855–68.

35. Mager DE, Jusko WJ. General pharmacokinetic model for drugs exhibiting target-mediated drug disposition. J Pharmacokinet Pharmacodyn. 2001;28:507–32.

36. Dua P, Hawkins E, Van Der Graaf P. A tutorial on target-mediated drug disposition (TMDD) models. CPT Pharmacomet Syst Pharmacol. 2015;4:324–37.

37. Sharma A, Jusko WJ. Characteristics of indirect pharmacodynamic models and applications to clinical drug responses. Br J Clin Pharmacol. 1998;45:229–39.

38. Mahmood I, Pettinato M. Impact of intrinsic and extrinsic factors on the pharmacokinetics of peptides: when is the assessment of certain factors warranted? Antibodies (Basel). 2021;11:1.

39. Delyon B, Lavielle M, Moulines E. Convergence of a stochastic approximation version of the EM algorithm. Ann Statist. 1999;27:94–128.

40. Ayral G, Si Abdallah JF, Magnard C, Chauvin J. A novel method based on unbiased correlations tests for covariate selection in nonlinear mixed effects models: the COSSAC approach. CPT Pharmacomet Syst Pharmacol. 2021;10:318–29.

41. Upton R, Mould D. Basic concepts in population modeling, simulation, and model-based drug development: part 3-introduction to pharmacodynamic modeling methods. CPT Pharmacomet Syst Pharmacol. 2014;3:88.

42. Le Douce J, Delétage N, Bourdès V, Lemarchant S, Godfrin Y. Subcommissural organ-spondin-derived peptide restores memory in a mouse model of Alzheimer's disease. Front Neurosci. 2021;15: 651094.

43. Greene C, Hanley N, Campbell M. Claudin-5: gatekeeper of neurological function. Fluids Barriers CNS. 2019;16:3.

44. Tachibana K, Hirayama R, Sato N, et al. Association of plasma claudin-5 with age and Alzheimer disease. Int J Mol Sci. 2024;25:1419.

45. Annunziata P, Cioni C, Masi G, Tassi M, Marotta G, Severi S. Fingolimod reduces circulating tight-junction protein levels and in vitro peripheral blood mononuclear cells migration in multiple sclerosis patients. Sci Rep. 2018;8:15371.

46. Beard RS Jr, Reynolds JJ, Bearden SE. Hyperhomocysteinemia increases permeability of the blood-brain barrier by NMDA receptor-dependent regulation of adherens and tight junctions. Blood. 2011;118:2007–14.

47. Tawfik A, Elsherbiny NM, Zaidi Y, Rajpurohit P. Homocysteine and age-related central nervous system diseases: role of inflammation. Int J Mol Sci. 2021;22:6259.

48. Xu R, Huang F, Wang Y, Liu Q, Lv Y, Zhang Q. Gender- and age-related differences in homocysteine concentration: a cross-sectional study of the general population of China. Sci Rep. 2020;10:17401.

49. Llewellyn DJ, Langa KM, Friedland RP, Lang IA. Serum albumin concentration and cognitive impairment. Curr Alzheimer Res. 2010;7:91–6.

50. Levin J, Bötzel K, Giese A, Vogeser M, Lorenzl S. Elevated levels of methylmalonate and homocysteine in Parkinson's disease, progressive supranuclear palsy and amyotrophic lateral sclerosis. Dement Geriatr Cogn Disord. 2010;29:553–9.

51. Valentino F, Bivona G, Butera D, et al. Elevated cerebrospinal fluid and plasma homocysteine levels in ALS. Eur J Neurol. 2010;17:84–9.

52. Fan X, Zhang L, Li H, et al. Role of homocysteine in the development and progression of Parkinson's disease. Ann Clin Transl Neurol. 2020;7:2332–8.

53. Ansari R, Mahta A, Mallack E, Luo JJ. Hyperhomocysteinemia and neurologic disorders: a review. J Clin Neurol. 2014;10:281–8.

54. Sahin S, Aksungar FB, Topkaya AE, et al. Increased plasma homocysteine levels in multiple sclerosis. Mult Scler. 2007;13:945–6.

55. Pourhamzeh M, Moravej FG, Arabi M, et al. The roles of serotonin in neuropsychiatric disorders. Cell Mol Neurobiol. 2022;42:1671–92.

56. Campbell BM, Charych E, Lee AW, Möller T. Kynurenines in CNS disease: regulation by inflammatory cytokines. Front Neurosci. 2014;8:12.

57. Wang Y, Chen S, Tan J, et al. Tryptophan in the diet ameliorates motor deficits in a rotenone-induced rat Parkinson's disease model via activating the aromatic hydrocarbon receptor pathway. Brain Behav. 2021;11: e2226.

58. Sandyk R, Fisher H. L-tryptophan supplementation in Parkinson's disease. Int J Neurosci. 1989;45:215–9.

59. Porter RJ, Lunn BS, Walker LL, Gray JM, Ballard CG, O'Brien JT. Cognitive deficit induced by acute tryptophan depletion in patients with Alzheimer's disease. Am J Psychiatry. 2000;157:638–40.

60. Bridel C, van Wieringen WN, Zetterberg H, et al. Diagnostic value of cerebrospinal fluid neurofilament light protein in neurology: a systematic review and meta-analysis. JAMA Neurol. 2019;76:1035–48.

61. Alagaratnam J, von Widekind S, De Francesco D, et al. Correlation between CSF and blood neurofilament light chain protein: a systematic review and meta-analysis. BMJ Neurol Open. 2021;3: e000143.

62. Meeker KL, Butt OH, Gordon BA, et al. Cerebrospinal fluid neurofilament light chain is a marker of aging and white matter damage. Neurobiol Dis. 2022;166: 105662.

63. Kaeser SA, Lehallier B, Thinggaard M, et al. A neuronal blood marker is associated with mortality in old age. Nat Aging. 2021;1:218–25.

64. Huang F, Zhu Y, Hsiao-Nakamoto J, et al. Longitudinal biomarkers in amyotrophic lateral sclerosis. Ann Clin Transl Neurol. 2020;7:1103–16.

65. Pawlitzki M, Schreiber S, Bittner D, et al. CSF neurofilament light chain levels in primary progressive MS: signs of axonal neurodegeneration. Front Neurol. 2018;9:1037.

66. Chen G, Xu J, Luo H, et al. Hevin/Sparcl1 drives pathological pain through spinal cord astrocyte and NMDA receptor signaling. JCI Insight. 2022;7: e161028.

67. Jayakumar AR, Apeksha A, Norenberg MD. Role of matricellular proteins in disorders of the central nervous system. Neurochem Res. 2017;42:858–75.

68. Bridel C, Koel-Simmelink MJA, Peferoen L, et al. Brain endothelial cell expression of SPARCL-1 is specific to chronic multiple sclerosis lesions and is regulated by inflammatory mediators in vitro. Neuropathol Appl Neurobiol. 2018;44:404–16.

69. Seddighi S, Varma VR, An Y, et al. SPARCL1 accelerates symptom onset in Alzheimer's disease and influences brain structure and function during aging. J Alzheimers Dis. 2018;61:401–14.

70. Haarmann A, Nowak E, Deiß A, et al. Soluble VCAM-1 impairs human brain endothelial barrier integrity via integrin α-4-transduced outside-in signalling. Acta Neuropathol. 2015;129:639–52.

71. Patel RB, Colangelo LA, Bielinski SJ, et al. Circulating vascular cell adhesion molecule-1 and incident heart failure: the Multi-Ethnic Study of Atherosclerosis (MESA). J Am Heart Assoc. 2020;9: e019390.

72. Perner C, Perner F, Gaur N, et al. Plasma VCAM1 levels correlate with disease severity in Parkinson's disease. J Neuroinflammation. 2019;16:94.

73. Cao MC, Cawston EE, Chen G, et al. Serum biomarkers of neuroinflammation and blood-brain barrier leakage in amyotrophic lateral sclerosis. BMC Neurol. 2022;22:216.

74. Chen T, Dai Y, Hu C, et al. Cellular and molecular mechanisms of the blood-brain barrier dysfunction in neurodegenerative diseases. Fluids Barriers CNS. 2024;21:60.